Electronic Supplementary Material (ESI) for Sustainable Energy & Fuels.

Supporting Information

Sequential and Simultaneous Ion Transfer into Carbon Nanopores during Charge–Discharge Cycles in Electrical Double-layer Capacitors

Hiroki Takamatsu,[†] Md Sharif Khan,[†] Takuya Araki,[‡] Chiharu Urita,[‡] Koki Urita,[‡] and Tomonori Ohba[†,]*

[†] Graduate School of Science, Chiba University, 1-33 Yayoi, Inage, Chiba 263-8522, Japan

[‡] Graduate School of Engineering, Nagasaki University, 1-14 Bunkyo, Nagasaki 852-8521, Japan

[*] E-mail: ohba@chiba-u.jp

Table S1–S3

Figure S1–S23

Table S1. Unit cell size of each system.

System	L_x / nm	L_y / nm	L_z / nm
0.98 nm wedge	5.18	5.10	14.51
1.5 nm wedge	5.13	5.10	14.42
2.3 nm wedge	5.26	5.10	14.45
2.9 nm wedge	5.12	5.10	14.48
3.4 nm wedge	5.19	5.10	14.45
1.7 nm slit	5.18	5.10	14.51
2.5 nm slit	5.18	5.10	14.51
3.2 nm slit	5.67	5.10	14.51
4.9 nm slit	7.39	5.10	14.51
Bulk	5.00	5.00	5.00

Table S2. The number of molecular species.

System	Lithium ion	Perchlorate ion	PC
0.98 nm wedge	85	85	879
1.5 nm wedge	99	99	1070
2.3 nm wedge	124	124	1358
2.9 nm wedge	135	135	1508
3.4 nm wedge	149	149	1654
1.7 nm slit	107	107	1178
2.5 nm slit	131	131	1441
3.2 nm slit	160	160	1776
4.9 nm slit	236	236	2610
Bulk	75	75	810

Table S3. Simulation parameters.

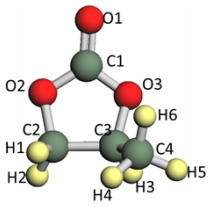

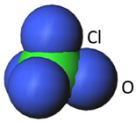

Lennard-Jones parameters and charges

Atom	ε / kJ mol^{-1}	σ / nm	q / e
C1	0.36	0.34	+0.8467
O1	0.88	0.30	-0.5525
O2	0.71	0.30	-0.4059
O3	0.71	0.30	-0.4069
C2	0.46	0.34	+0.0964
C3	0.46	0.34	+0.1121
C4	0.46	0.34	-0.1111
H1, H2	0.066	0.25	+0.0797
H3	0.066	0.25	+0.0857
H4, H5, H6	0.066	0.26	+0.0587
Li	0.69	0.15	+1.0000
Cl	1.1	0.35	+1.0120
O	0.88	0.30	-0.5030
Pore carbon	0.36	0.34	-

Improper coefficients

Improper	$K_{improper}$ / kJ	n	d
O3-C1-O2-O1	43.9	2	-1

Bond coefficients

Bond	K_{bond} / 10^3 kJ nm^{-2}	r / nm
C1-O1	271	0.1214
C1-O2	172	0.1343
C1-O3	172	0.1343
O2-C2	126	0.1439
O3-C3	126	0.1439
C2-C3	127	0.1535
C2-H1	140	0.1093
C2-H2	140	0.1093
C3-H3	140	0.1093
C3-C4	127	0.1535
C4-H4	141	0.1092
C4-H5	141	0.1092
C4-H6	141	0.1092
Cl-O	233	0.1483

Angle coefficients

Angle	K_{angle} / kJ radian^2	Θ / degrees
C1-O2-C2	266	115.14
C1-O3-C3	266	115.14
O1-C1-O2	317	123.33
O1-C1-O3	317	123.33
O2-C1-O3	319	111.38
O2-C2-C3	283	108.42
O2-C2-H1	212	108.82
O2-C2-H2	212	108.82
O3-C3-C2	283	108.42
O3-C3-H3	212	108.82
O3-C3-C4	283	108.42
C2-C3-H3	193	110.07
C2-C3-C4	264	110.63
C3-C2-H1	194	110.07
C3-C2-H2	194	110.07
C3-C4-H4	194	110.05
C3-C4-H5	194	110.05
C3-C4-H6	194	110.05
H3-C3-C4	194	110.07
H1-C2-H2	164	109.55
H4-C4-H5	165	108.35
H4-C4-H6	165	108.35
H5-C4-H6	165	108.35
O-Cl-O	586	109.47

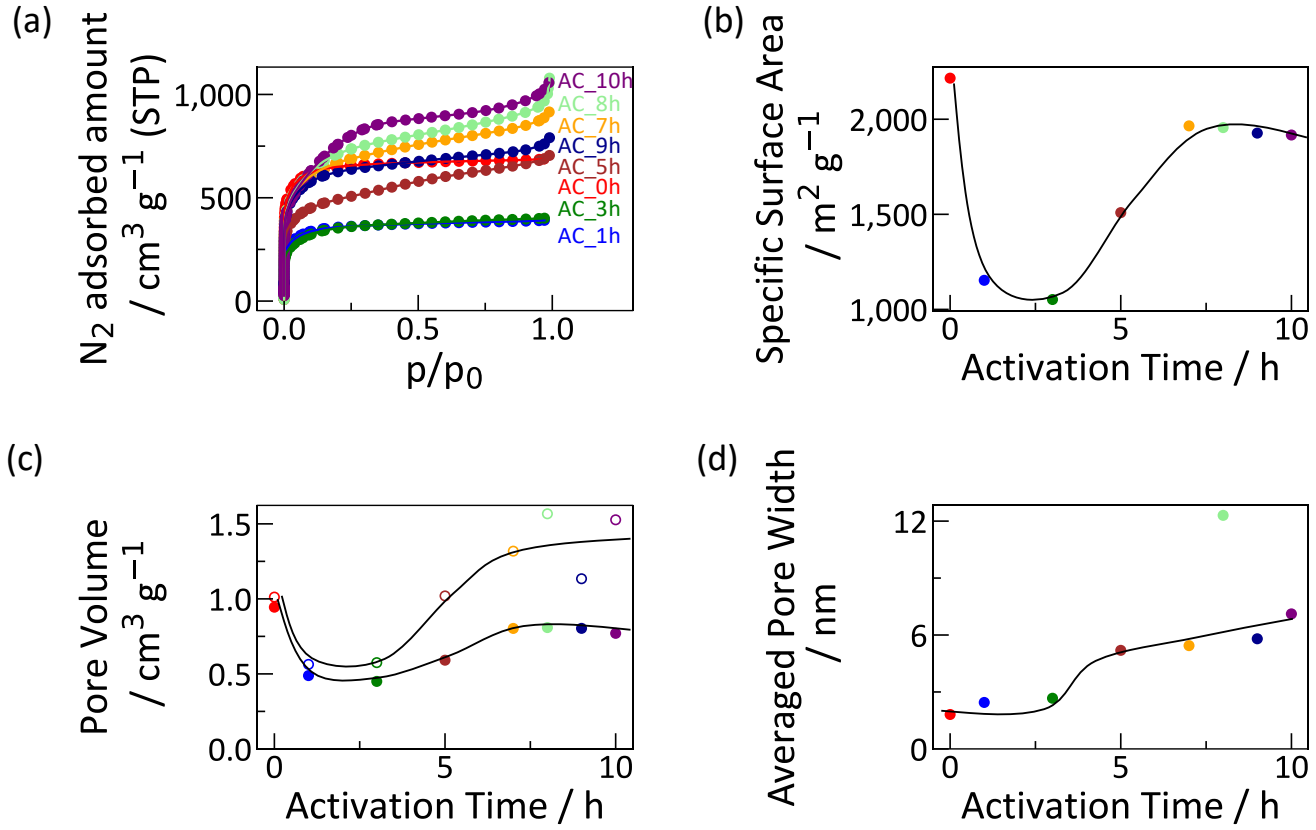

Figure S1. Pore structure evaluation of activated carbons by N_2 adsorption isotherms at 77 K (a). Specific surface area (b), micropore and total pore volumes (c), and averaged pore width (d) as a function of activation time of carbon samples. Filled and open symbols, respectively, depicted micropore, and total pore volumes.

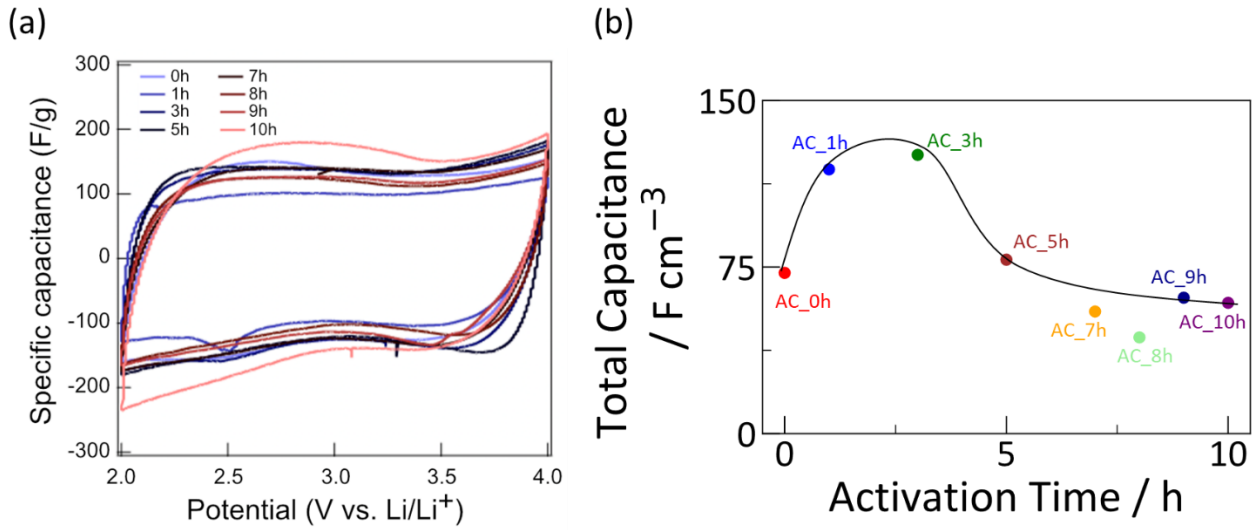

Figure S2. Capacitance dependence on activation time. (a) CV curves. (b) Total capacitance normalized by the total pore volume of ACs determined from N_2 adsorption isotherm.

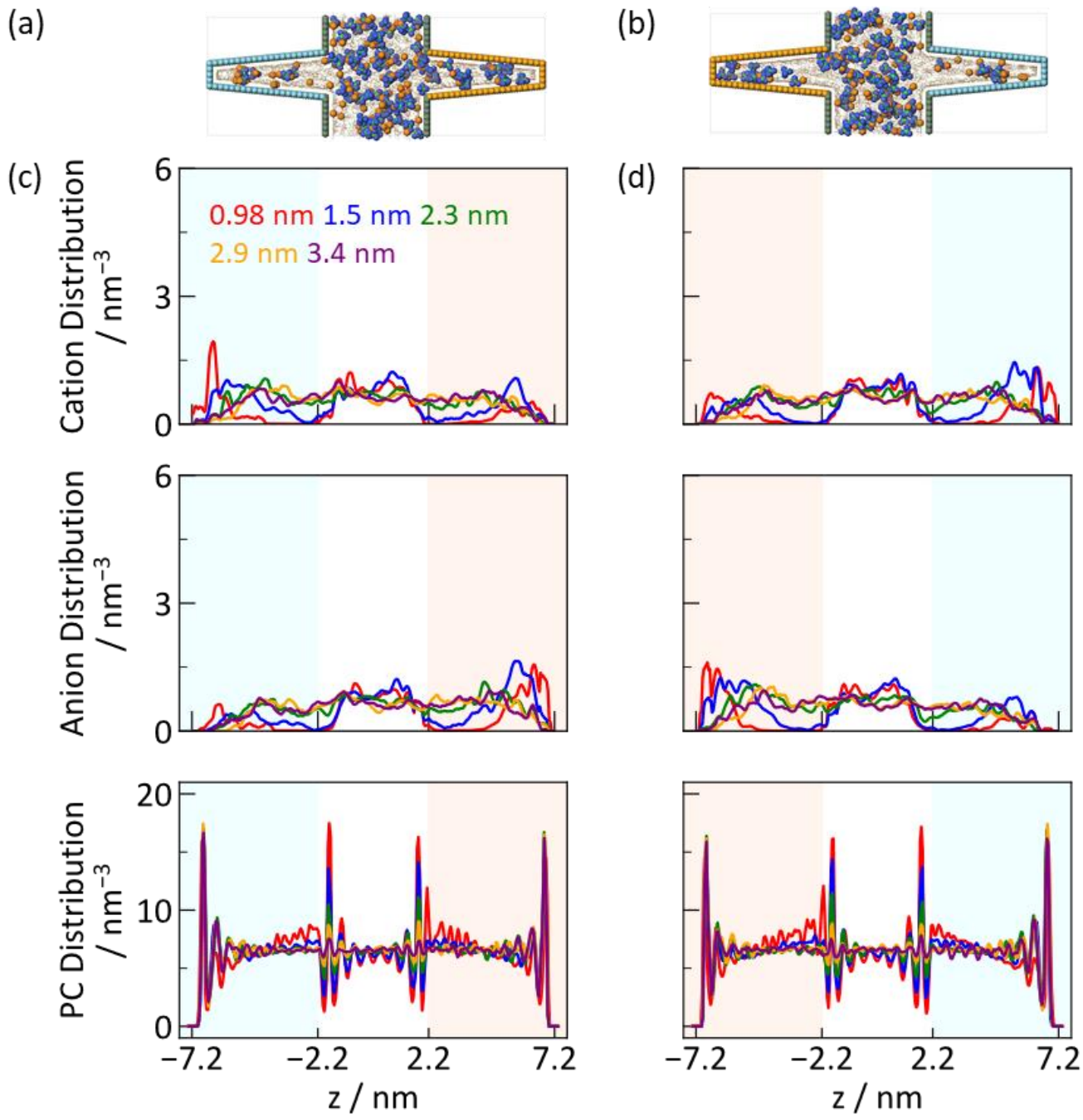

Figure S3. Snapshots of ions in wedge-shaped pores with a positive charge (+0.01 e) on the right side carbons and negative charge (−0.01 e) on left side carbons (a), and negative charges on the right side carbons and positive charges on left side carbons (b) applying charges of ±0.01 e in the wedge-shaped pores with the averaged pore size of 0.98, 1.5, 2.3, 2.9, and 3.4 nm. Orange and blue spheres, gray ball-and-stick represent Li^+ and ClO_4^- ions, and PC, respectively. (c, d) Cationic (top), anionic (middle), and PC (bottom) distributions against z-direction in the partial condition of (a) and (b), respectively.

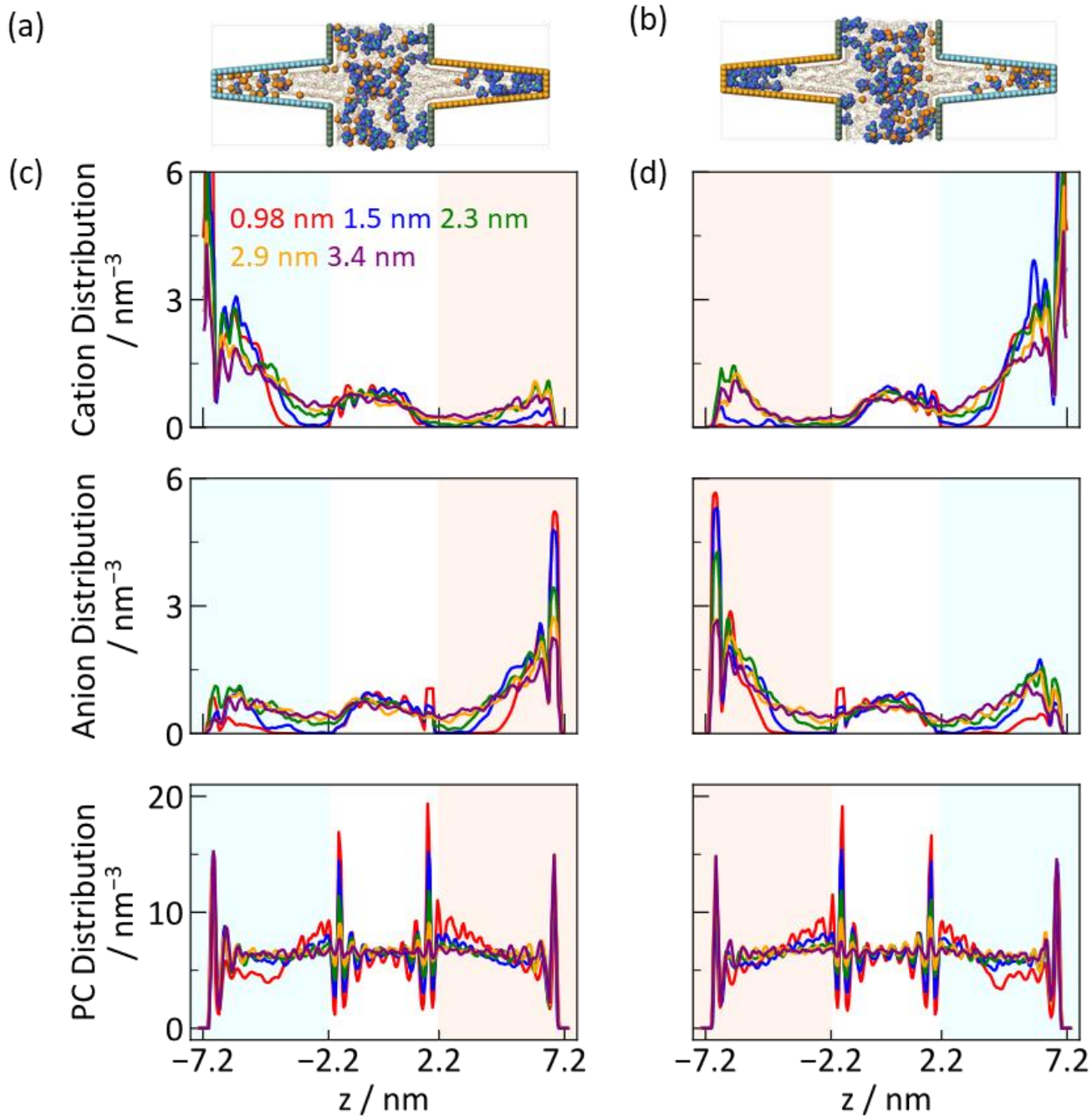

Figure S4. Snapshots of ions in wedge-shaped pores with a positive charge (+0.02 e) on the right side carbons and negative charge (−0.02 e) on left side carbons (a), and negative charges on the right side carbons and positive charges on left side carbons (b) applying charges of ±0.02 e in the wedge-shaped pores with the averaged pore size of 0.98, 1.5, 2.3, 2.9, and 3.4 nm. Orange and blue spheres, gray ball-and-stick represent Li^+ and ClO_4^- ions, and PC, respectively. (c, d) Cationic (top), anionic (middle), and PC (bottom) distributions against z-direction in the partial condition of (a) and (b), respectively.

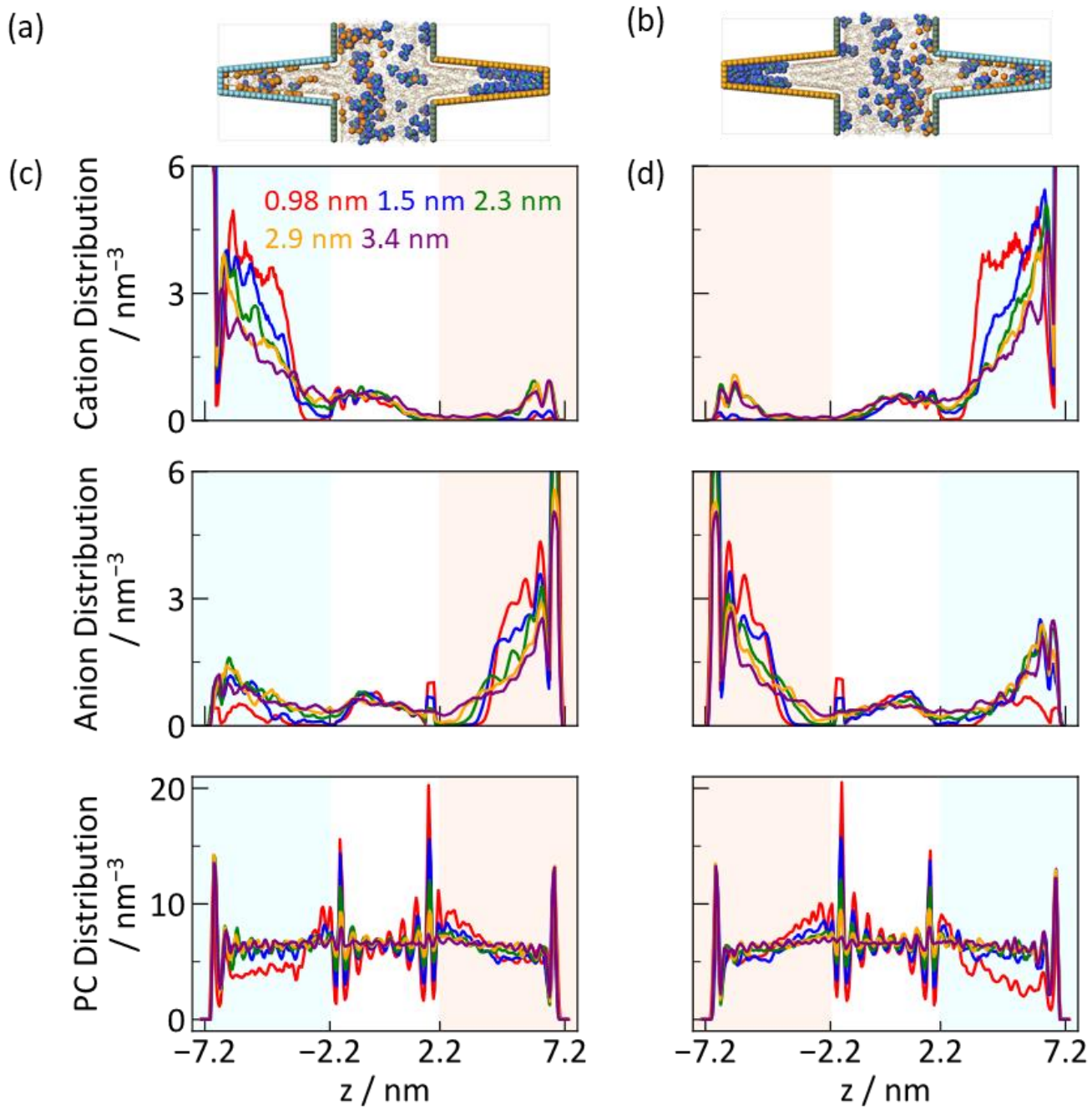

Figure S5. Snapshots of ions in wedge-shaped pores with a positive charge (+0.03 e) on the right side carbons and negative charge (−0.03 e) on left side carbons (a), and negative charges on the right side carbons and positive charges on left side carbons (b) applying charges of ±0.03 e in the wedge-shaped pores with the averaged pore size of 0.98, 1.5, 2.3, 2.9, and 3.4 nm. Orange and blue spheres, gray ball-and-stick represent Li^+ and ClO_4^- ions, and PC, respectively. (c, d) Cationic (top), anionic (middle), and PC (bottom) distributions against z-direction in the partial condition of (a) and (b), respectively.

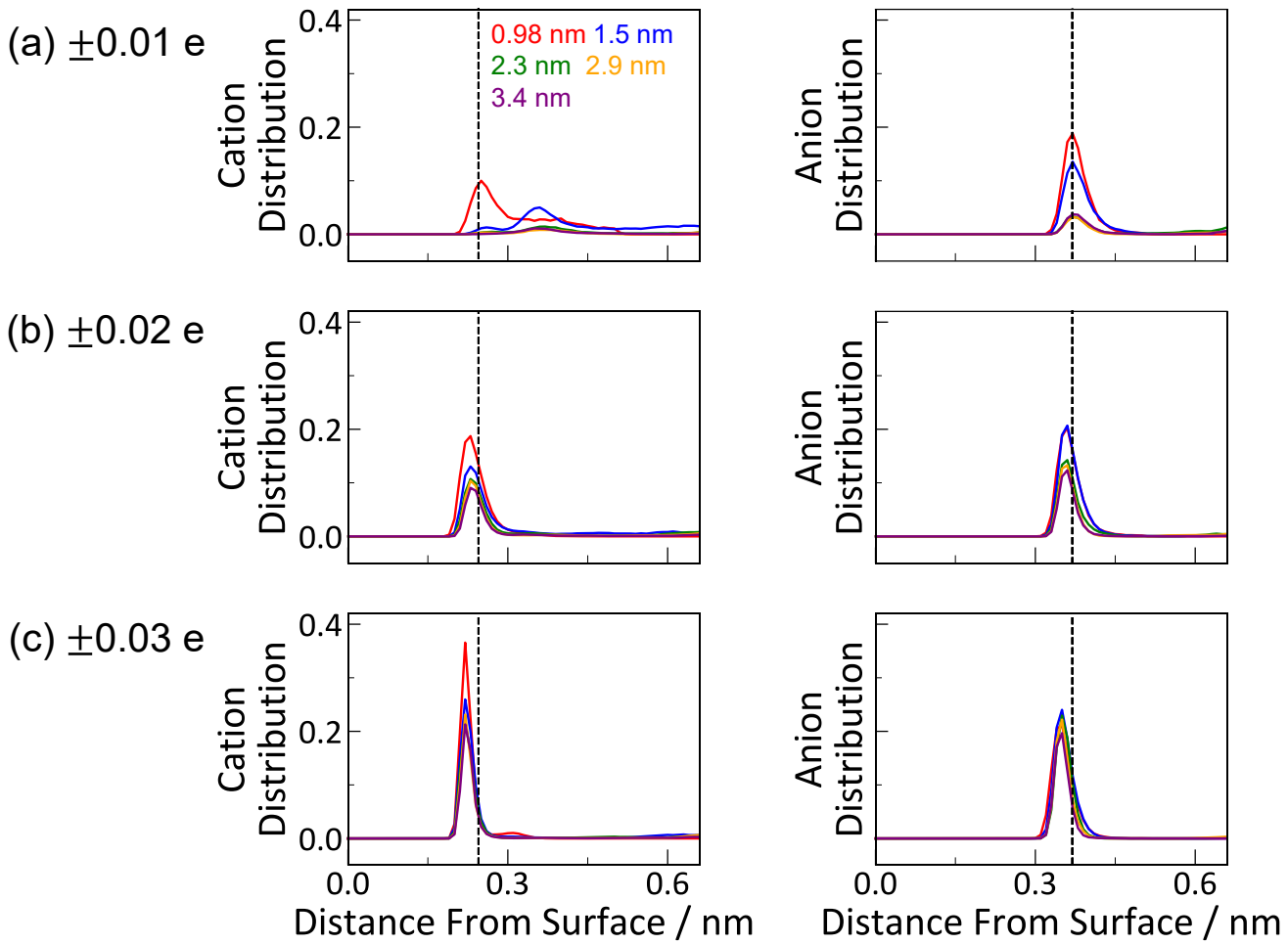

Figure S6. Distribution of distance between a cation and a carbon atom (left), and an anion and a carbon atom (right) under applying a charge of ±0.01 e (a), ±0.02 e (b), and ±0.03 e (c) in the wedge-shaped pores with the averaged pore size of 0.98, 1.5, 2.3, 2.9, and 3.4 nm. Collision distances are 0.26 and 0.37 nm for cation–carbon and anion–carbon, respectively, which are shown in the black dashed line.

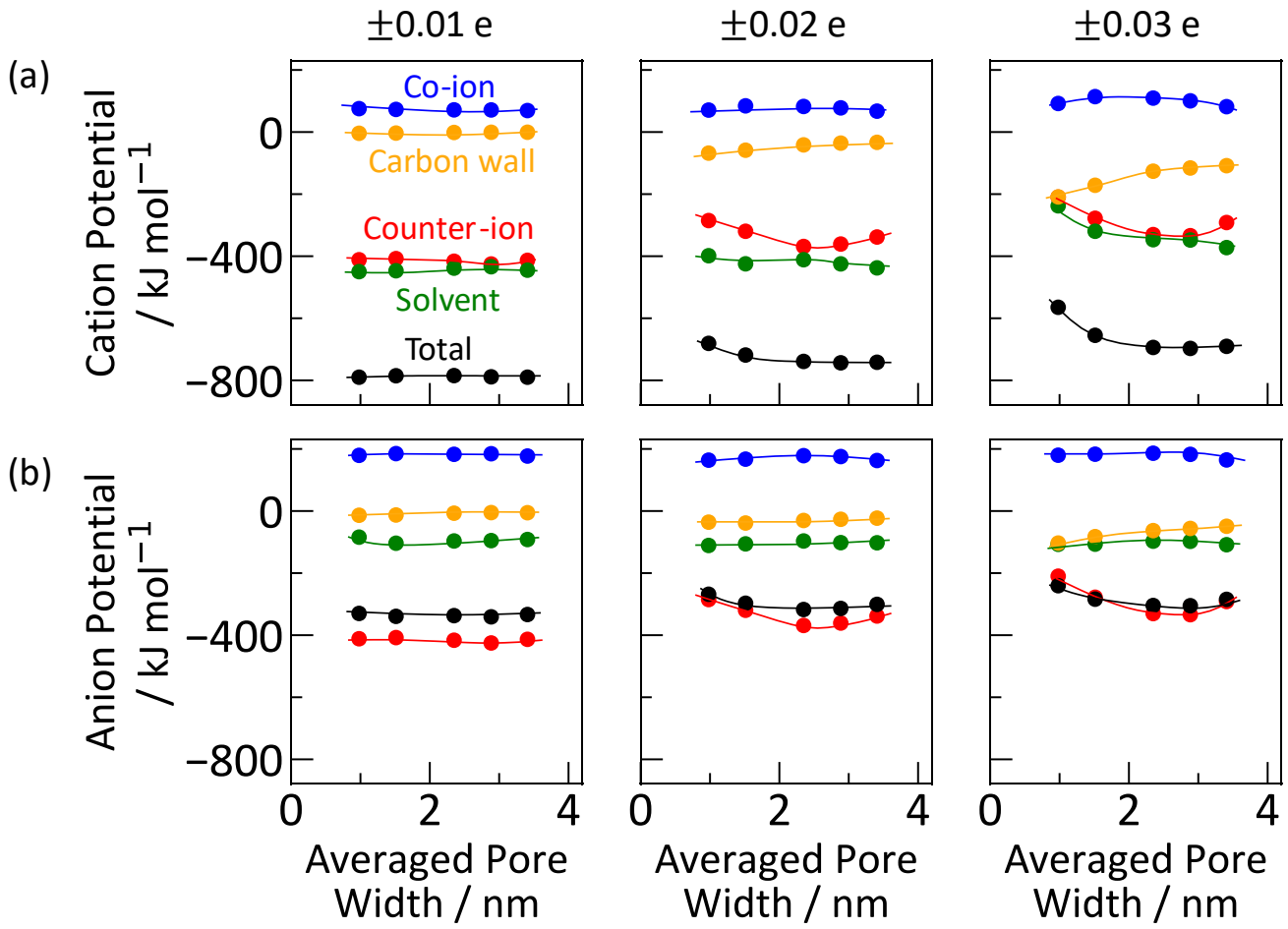

Figure S7. (a) Cation potential from co-ion, carbon wall, counter-ion, and solvent. (b) Anion potential from co-ion, carbon wall, counter-ion, and solvent.

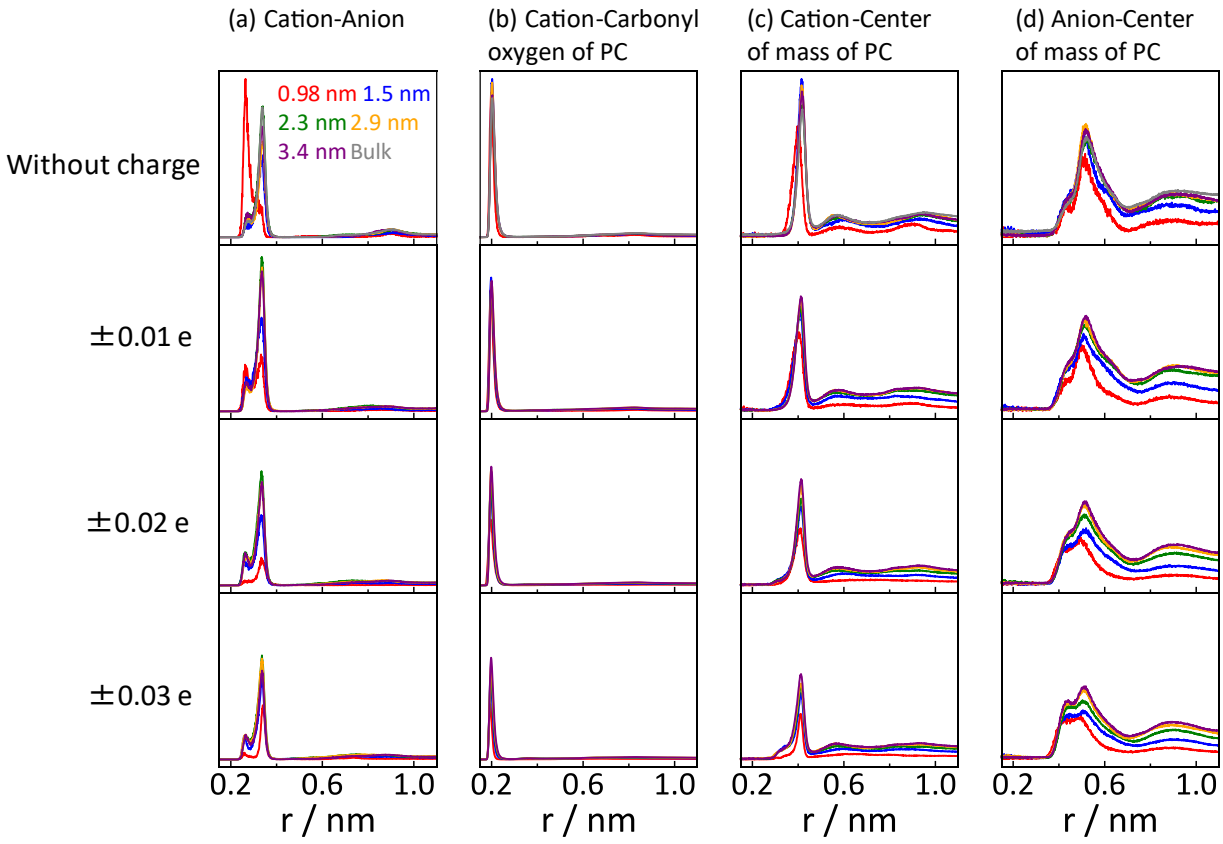

Figure S8. The radial distribution function of cation-anion (a), cation-carbonyl oxygen of PC (b), cation-center of mass of PC (c), and anion-PC (d) without charge (top), with ±0.01 e (second from top), ±0.02 e (second from bottom) and ±0.03 e (bottom) in the wedge-shaped pores with the averaged pore size of 0.98, 1.5, 2.3, 2.9, and 3.4 nm.

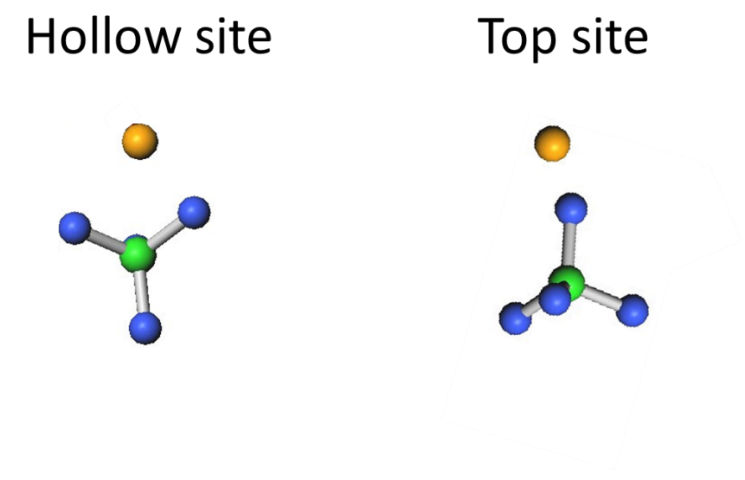

Figure S9. Snapshots of Li^+ (orange) at the hollow site and the top site of ClO_4^-.

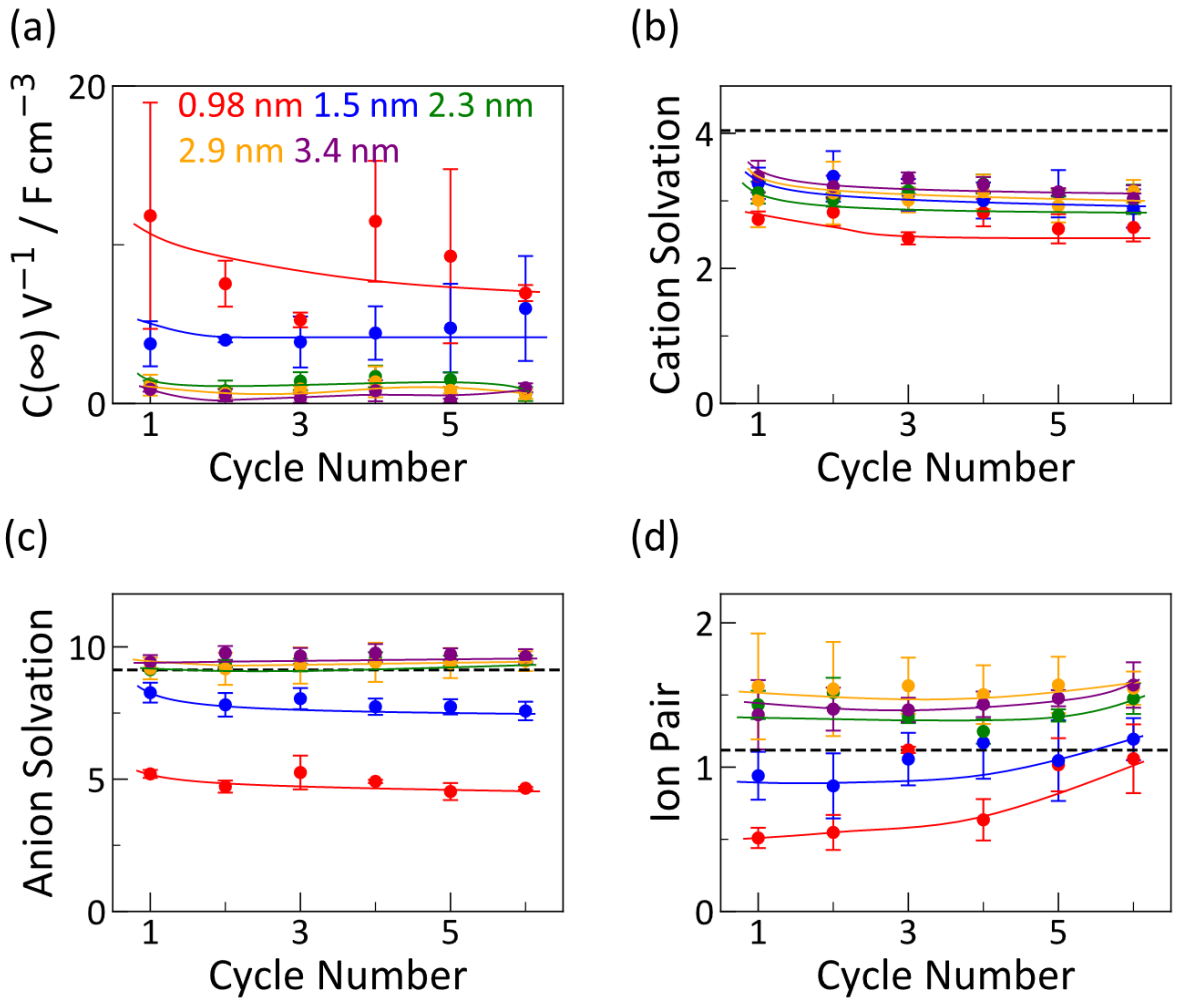

Figure S10. Cyclability for capacitance (a), cation solvation (b), anion solvation (c), and ion pair (d) under applying a charge of ±0.01 e in the wedge-shaped pores with the averaged pore size of 0.98, 1.5, 2.3, 2.9, and 3.4 nm. Ion pair and cation and anion solvations were calculated in the pores. Bulk solvation and ion pair numbers are shown in a black dashed line.

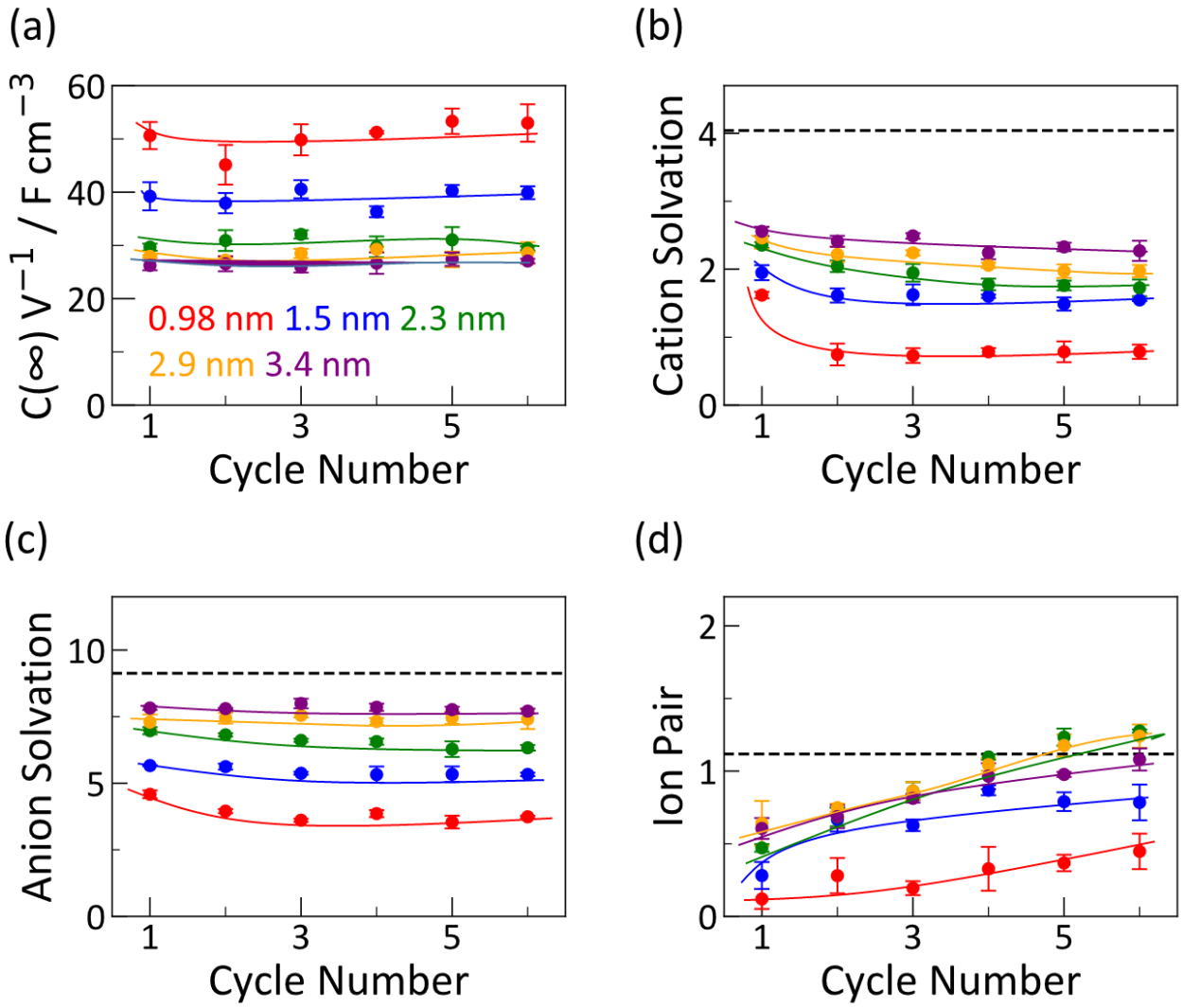

Figure S11. Cyclability for capacitance (a), cation solvation (b), anion solvation (c), and ion pair (d) under applying a charge of ±0.03 e in the wedge-shaped pores with the averaged pore size of 0.98, 1.5, 2.3, 2.9, and 3.4 nm. Ion pair and cation and anion solvations were calculated in the pores. Bulk solvation and ion pair numbers are shown in a black dashed line.

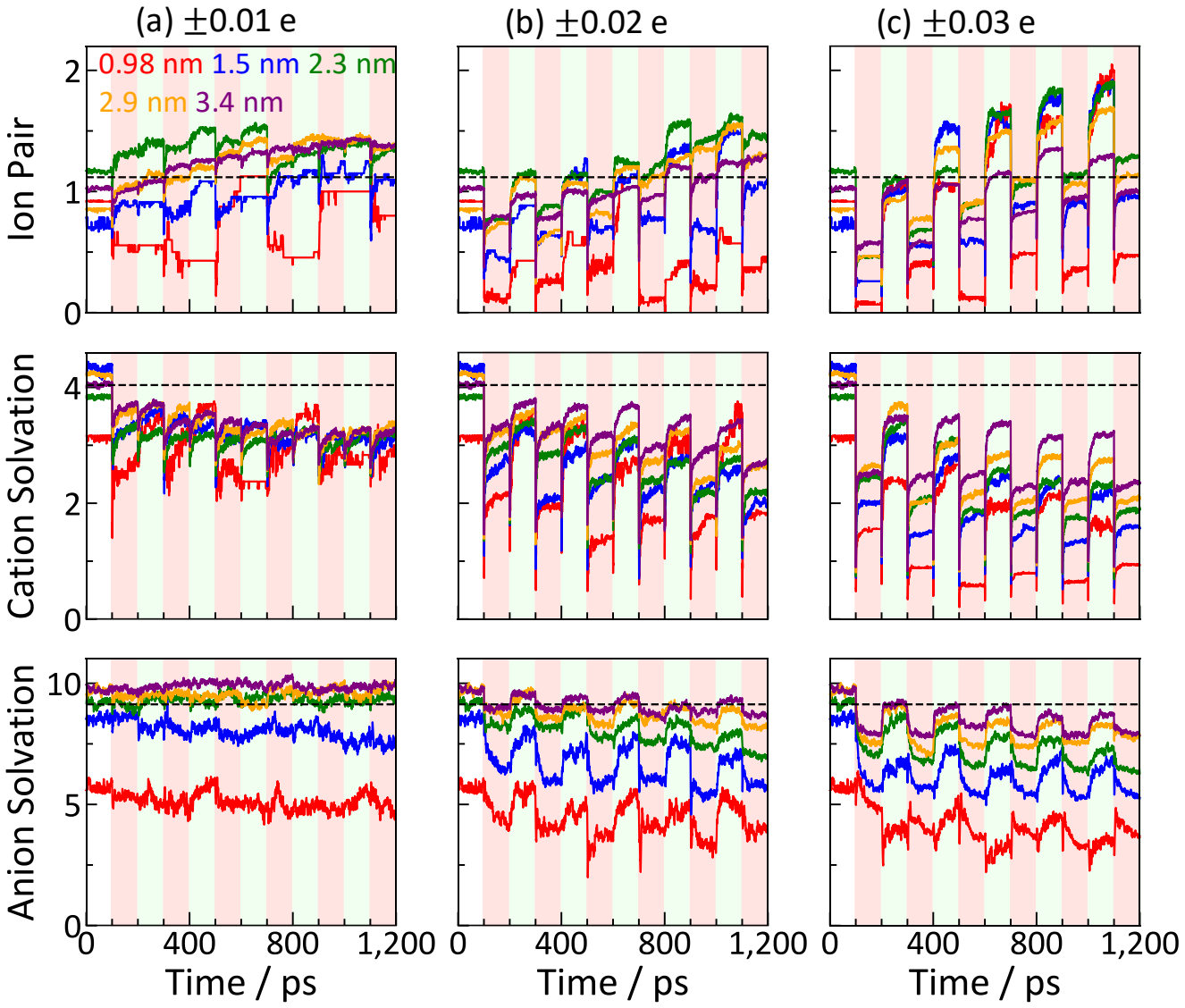

Figure S12. Ion pair and cation and anion solvation in the pores applying partial charges of ±0.01 e (a), ±0.02 e (b), and ±0.03 e (c) in the wedge-shaped pores with the averaged pore size of 0.98, 1.5, 2.3, 2.9, and 3.4 nm. Those in bulk were shown in a black dashed line. Red and green shades indicate charging and releasing, respectively.

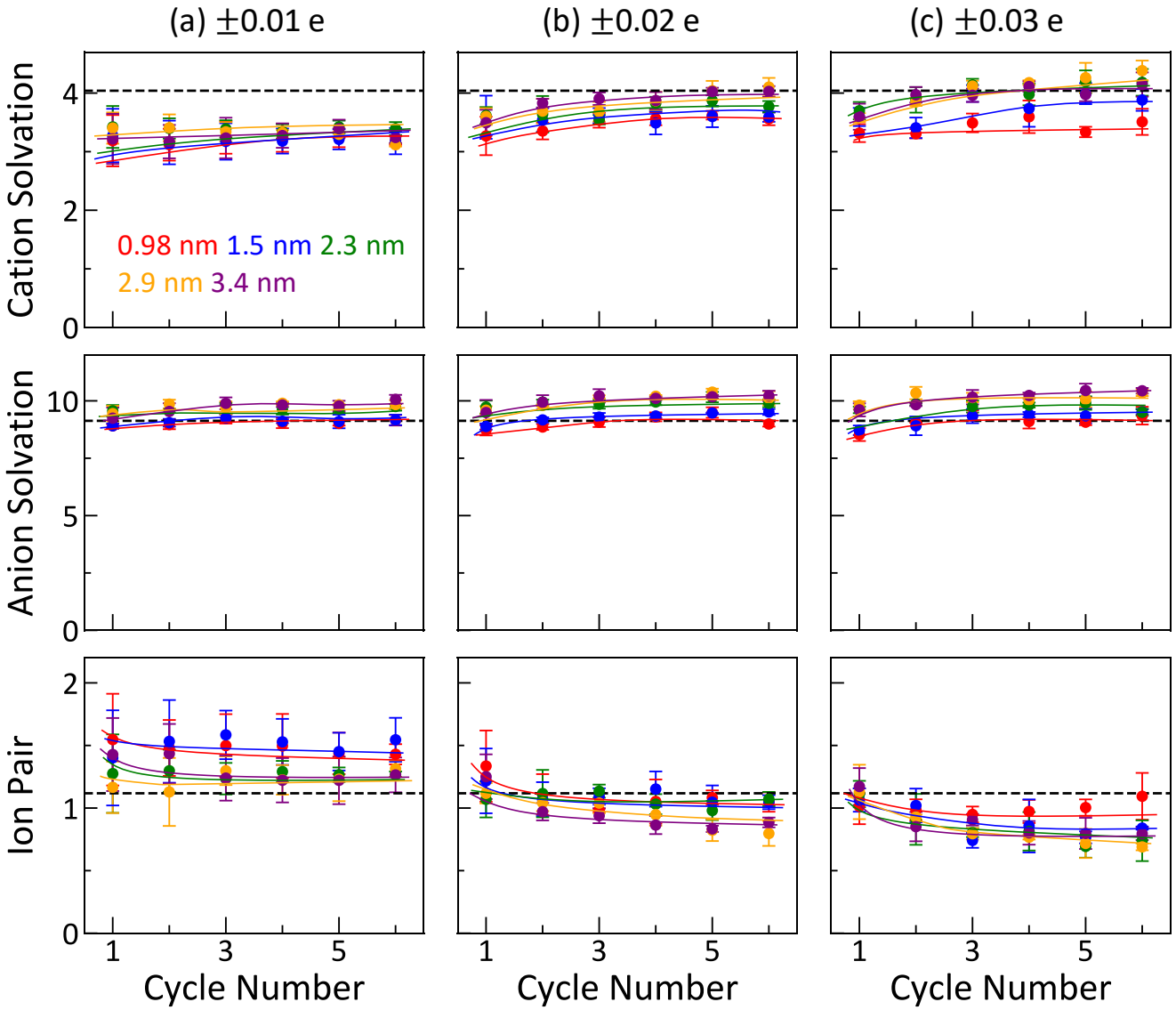

Figure S13. Cation and anion solvation and ion pair in inter-electrode space applying partial charges of ±0.01 e (a), ±0.02 e (b), and ±0.03 e (c) in the wedge-shaped pores with the averaged pore size of 0.98, 1.5, 2.3, 2.9, and 3.4 nm.

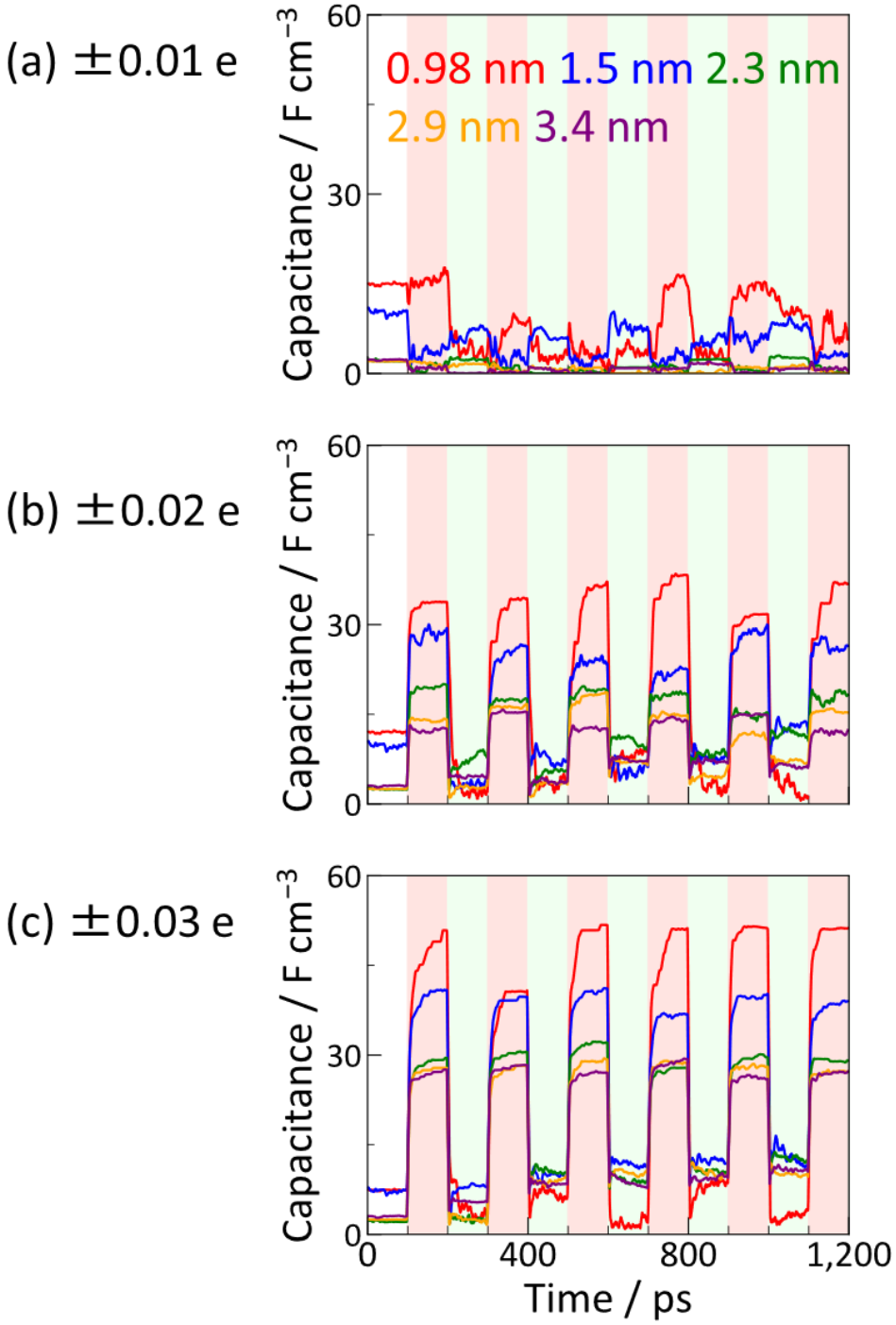

Figure S14. Capacitance at a charge of ±0.01 e (a), ±0.02 e (b), and ±0.03 e (c) in the wedge-shaped pores with the averaged pore size of 0.98, 1.5, 2.3, 2.9, and 3.4 nm.

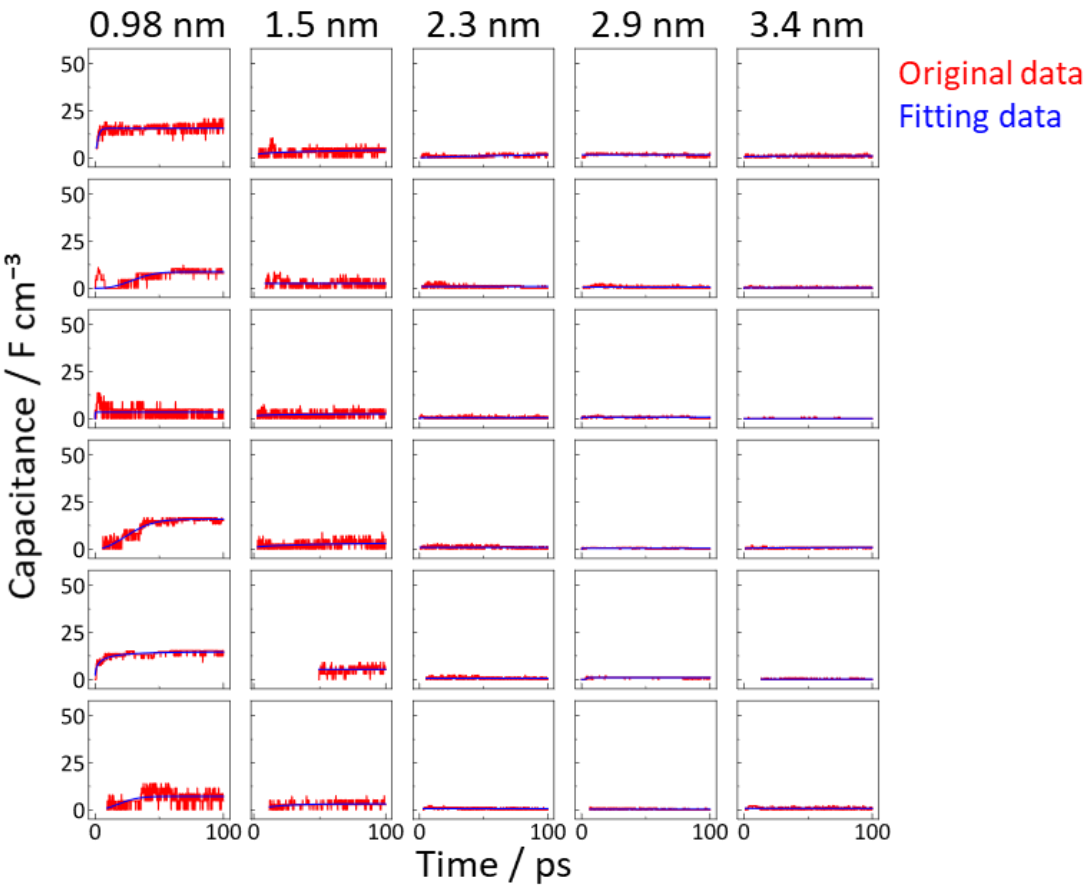

Figure S15. Curve fitting results of capacitance change during charging applying partial charges of ±0.01 e in the wedge-shaped pores with the averaged pore size of 0.98, 1.5, 2.3, 2.9, and 3.4 nm. From the top, the results are shown from the first to the fifth charging. Original data and fitting results are shown in red and blue, respectively.

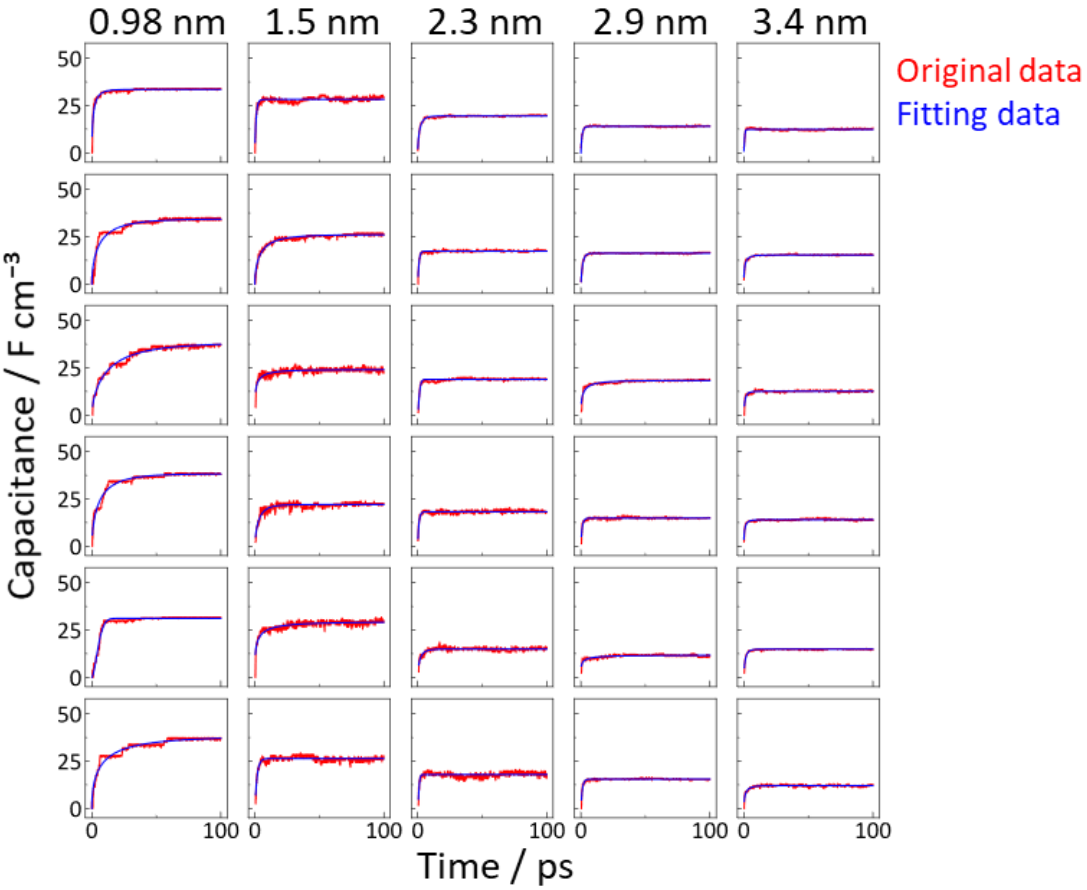

Figure S16. Curve fitting results of capacitance change during charging applying partial charges of ±0.02 e in the wedge-shaped pores with the averaged pore size of 0.98, 1.5, 2.3, 2.9, and 3.4 nm. From the top, the results are shown from the first to the fifth charging. Original data and fitting results are shown in red and blue, respectively.

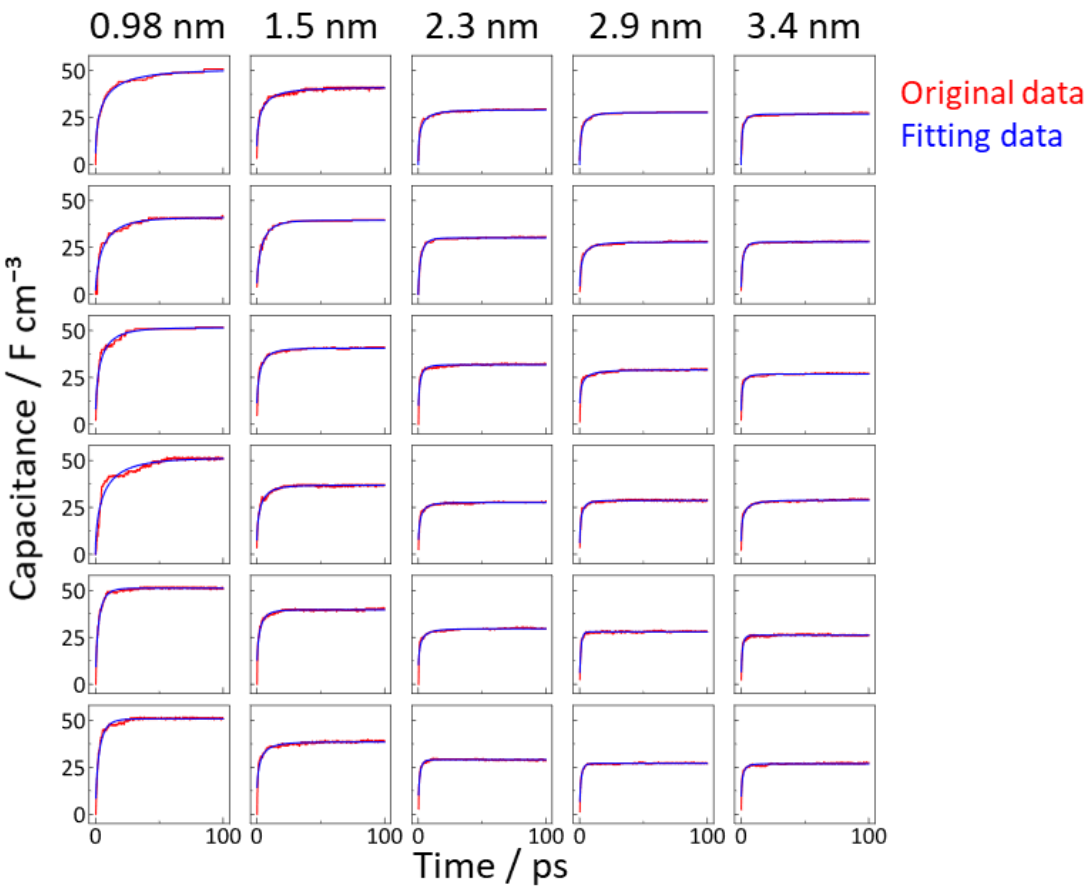

Figure S17. Curve fitting results of capacitance change during charging applying partial charges of ±0.03 e in the wedge-shaped pores with the averaged pore size of 0.98, 1.5, 2.3, 2.9, and 3.4 nm. From the top, the results are shown from the first to the fifth charging. Original data and fitting results are shown in red and blue, respectively.

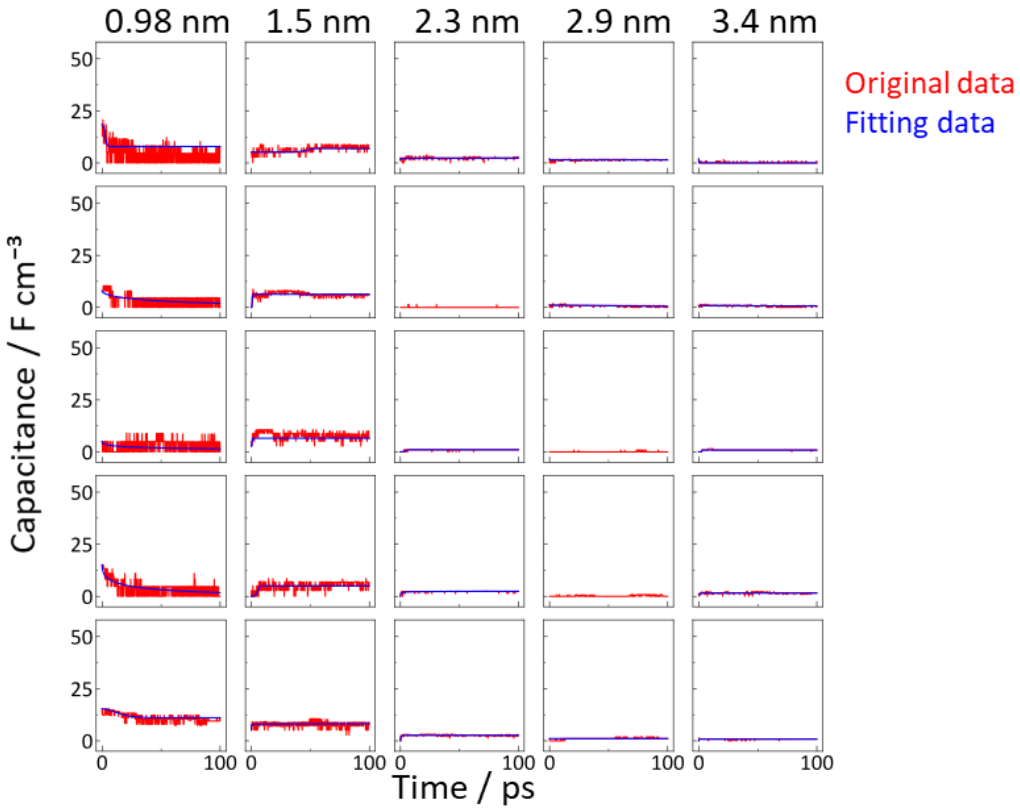

Figure S18. Curve fitting results of capacitance change during release, applying partial charges of ±0.01 e in the wedge-shaped pores with the averaged pore size of 0.98, 1.5, 2.3, 2.9, and 3.4 nm. From the top, the results are shown from the first to the fourth release. Original data and fitting results are shown in red and blue, respectively.

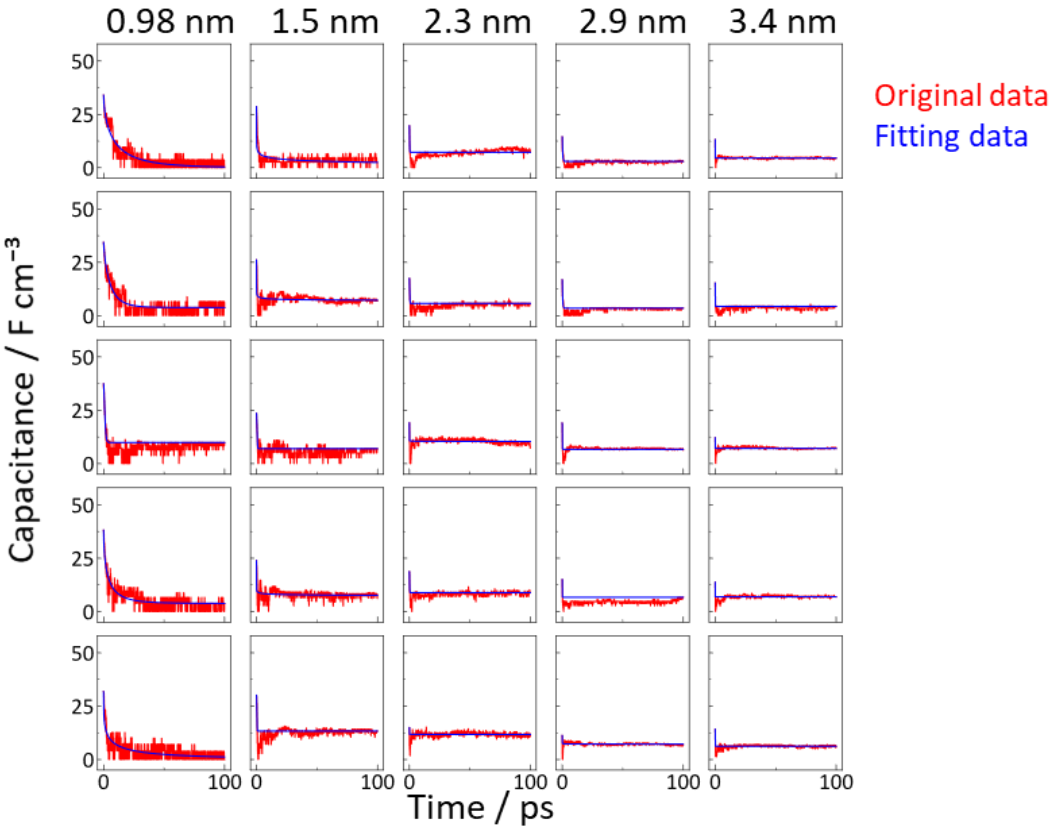

Figure S19. Curve fitting results of capacitance change during release, applying partial charges of ±0.02 e in the wedge-shaped pores with the averaged pore size of 0.98, 1.5, 2.3, 2.9, and 3.4 nm. From the top, the results are shown from the first to the fourth release. Original data and fitting results are shown in red and blue, respectively.

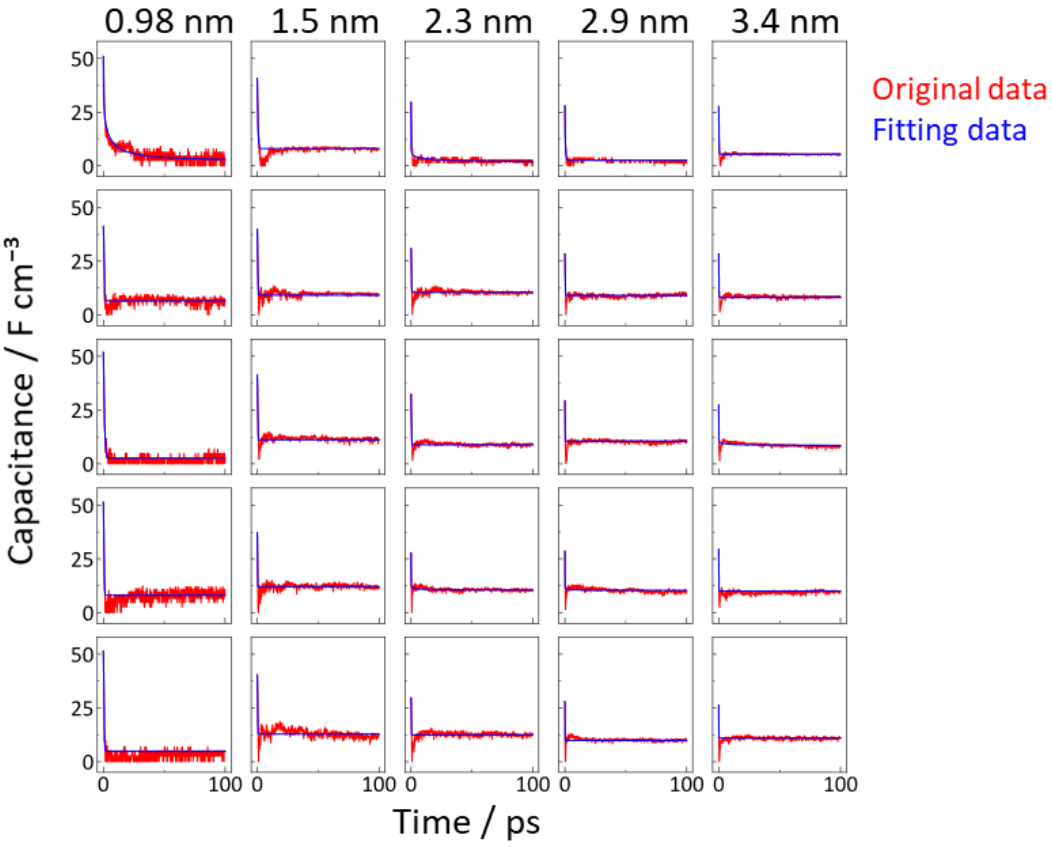

Figure S20. Curve fitting results of capacitance change during release, applying partial charges of ±0.03 e in the wedge-shaped pores with the averaged pore size of 0.98, 1.5, 2.3, 2.9, and 3.4 nm. From the top, the results are shown from the first to the fourth release. Original data and fitting results are shown in red and blue, respectively.

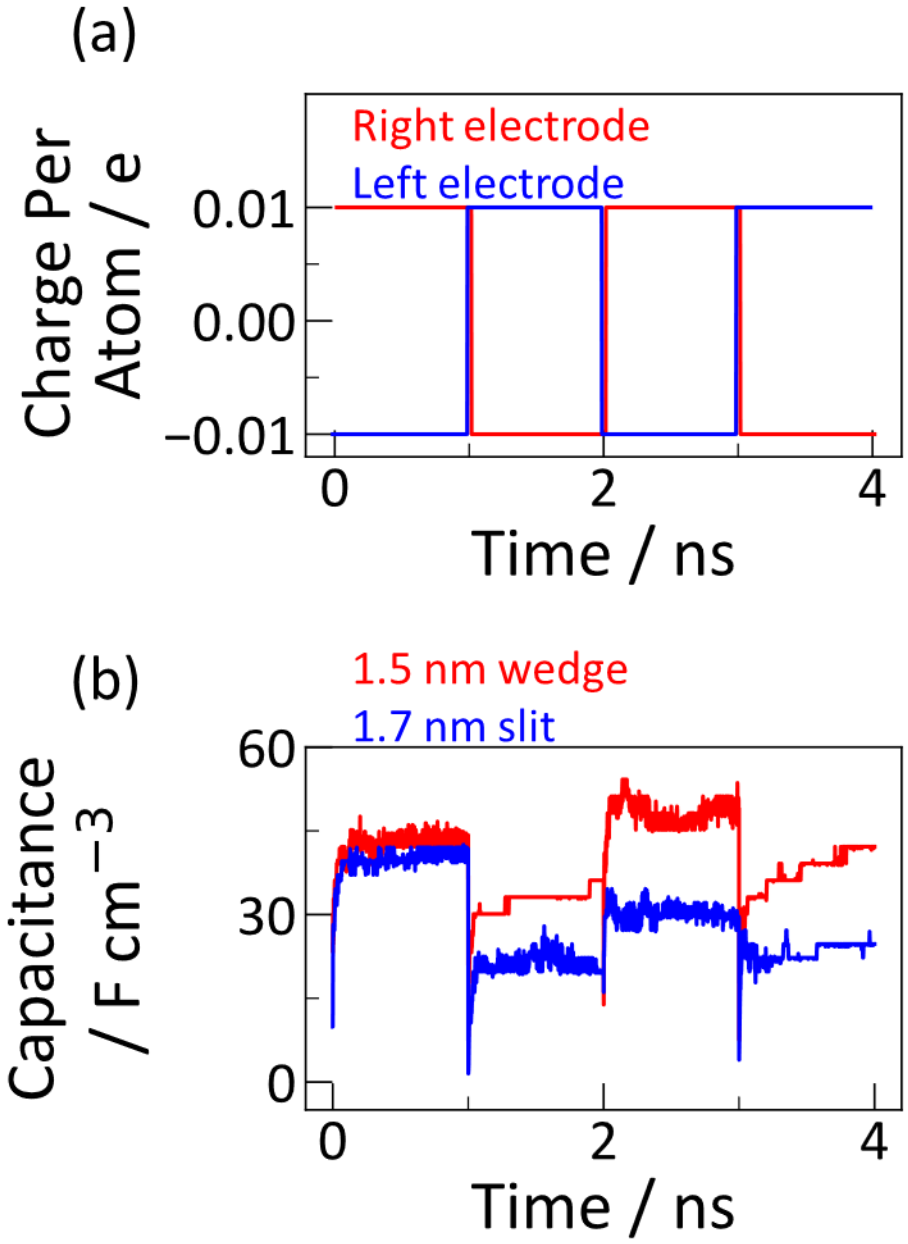

Figure S21. (a) Scheme of the partial charges on porous carbons of the right and left porous carbon electrodes with time progress. (b) Capacitance changes in long charge/release cycles at +0.01 e.

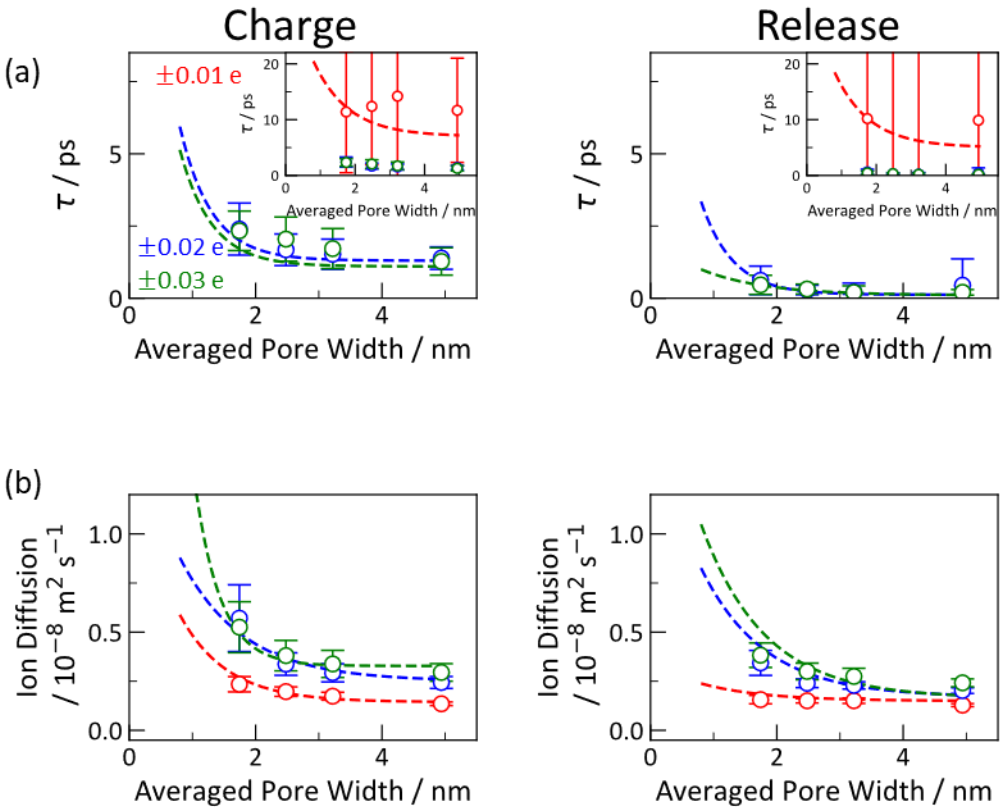

Figure S22. Mobility of ions under charge/release in slit pore. Dashed curves represent wedge curves. (a) The relaxation time of capacitances under charge and release. (b) Diffusion coefficient of ions under charge and release.

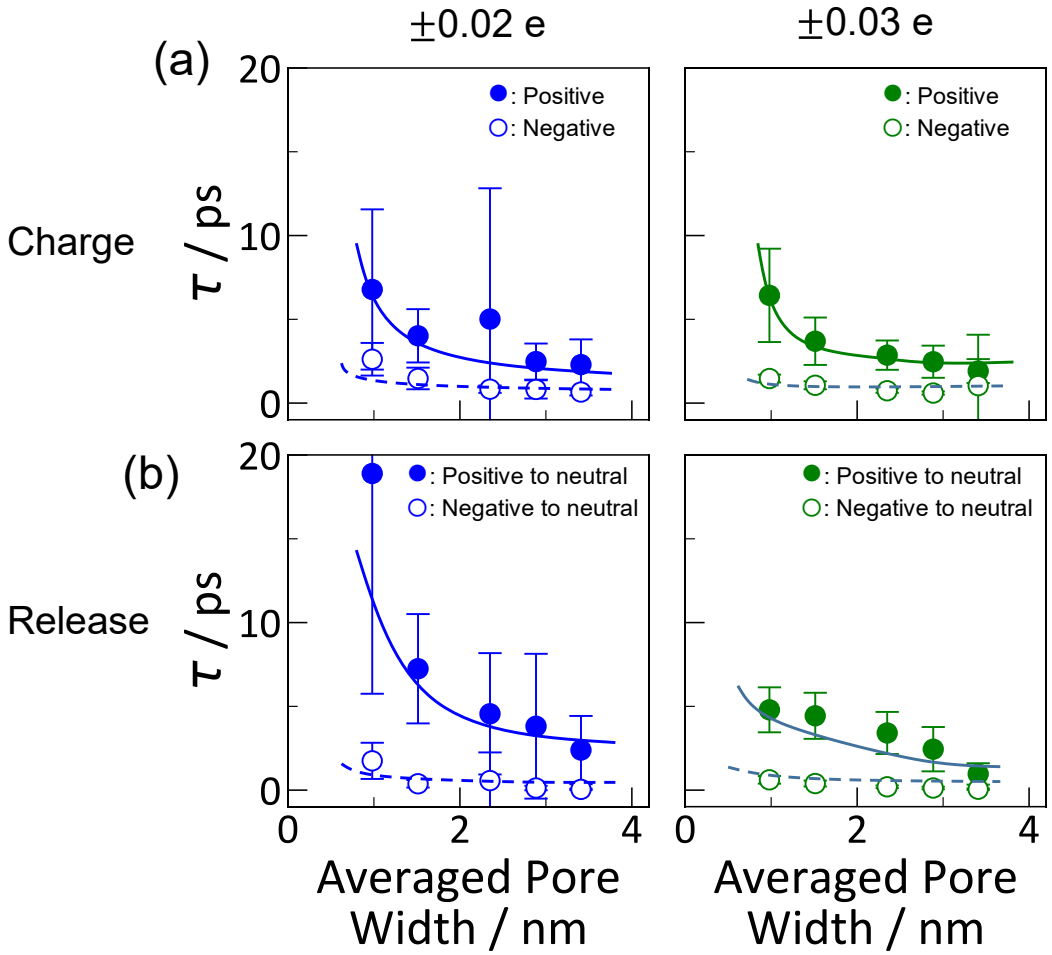

Figure S23. Relaxation time calculated using a single pore. (a) Relaxation time under positive charge (filled symbols and solid curves) and negative charge (open symbols and dashed curves). (b) Relaxation time under release positive to neutral represented by filled symbols with solid curves and negative to neutral represented by open symbols with dashed curves.